A Liénard Oscillator Resonant Tunnelling Diode-Laser Diode Hybrid Integrated Circuit: Model and Experiment

Thomas J. Slight, Bruno Romeira, *Student Member, IEEE*, Liquan Wang, José M. L. Figueiredo, Edward Wasige, *Member, IEEE*, and Charles N. Ironside, *Senior Member, IEEE*

Abstract—We report on a hybrid optoelectronic integrated circuit based on a resonant tunnelling diode driving an optical communications laser diode. This circuit can act as a voltage controlled oscillator with optical and electrical outputs. We show that the oscillator operation can be described by Liénard's equation, a second order nonlinear differential equation, which is a generalization of the Van der Pol equation. This treatment gives considerable insight into the potential of a monolithic version of the circuit for optical communication functions including clock recovery and chaotic source applications.

Index Terms—Driver circuits, integrated optoelectronics, nonlinear systems, optical fiber communication, oscillators, resonant tunneling diodes, semiconductor lasers, .

I. Introduction

RECENT work on Opto Electronic Integrated Circuits (OEICs) has shown that it is possible to monolithically integrate a resonant tunnelling diode (RTD) with an optical waveguide electroabsorption modulator (RTD-EAM) [1] and a RTD with a laser diode (RTD-LD) [2]. Crucially the RTD introduces negative differential resistance (NDR) into the electrical characteristics of the RTD-EAM and the RTD-LD.

In this paper we present a hybrid integrated RTD-LD circuit (the RTD-LD HIC) operating as an optoelectronic voltage controlled oscillator (VCO). RTD based VCOs have exhibited oscillation frequencies up to 470 GHz [3], however because of the physical layout of the RTD-LD HIC we are restricted to relatively low frequencies (< 10 GHz). With monolithically integrated circuits much higher frequency operation will be obtainable and the insights achieved with the hybrid circuit will be applicable at data rates more appropriate for current and future optical communication systems.

Simple circuits that include NDR components are generally described by the Van der Pol and Duffing equations [4]–[6], [3]. Considerable insight into the behaviour of NDR based circuits

has been achieved using the Van der Pol equation, originally formulated in the 1920s to describe oscillator circuits for radio systems that include NDR components [7]. The Van der Pol equation is a nonlinear second order differential equation and is an early example of a type of nonlinear differential equation that forms the foundation of chaos theory for dynamical systems. These equations have applications in many areas, they have been studied extensively and there exists a large body of literature on this topic—for review see [8]. However, we found that Van der Pol approach to our circuit does not allow a detailed description of the RTD-LD HIC voltage dependent current and hence the current flowing in the circuit. Here, we show that when a deeper insight is needed a more general approach based on the Liénard equation is necessary. The Liénard equation [9], which contains the special cases of the Van der Pol and Duffing equations, is used because it allows a more accurate description of the current versus voltage $(I–V)$ characteristic of the RTD based RTD-LD HIC. We also show for the first time how the theory of nonlinear differential equations can be applied to a driver circuit for an optical communications semiconductor laser. We anticipate that this circuit will lead to new applications in optical communications including clock recovery from oscillator entrainment, clock division and data encryption using synchronized chaotic behaviour.

The paper is organized as follows. The next section describes the circuit and the circuit components, the electrical equivalent circuit and the operating principle. In Section III, the theory of the RTD-LD HIC is presented with the corresponding numerical equations that describe the electrical and the optical behaviour. Section IV describes the experimental results in the electrical and optical domains and the comparison with the numerical predictions. Section V is devoted to the conclusions.

II. Circuit Description and Operating Principle

The physical layout of the RTD-LD HIC is shown in Fig. 1. The laser diode and the RTD are connected in series using a printed circuit board (PCB). A shunt capacitor $C_c (= 1\mu\text{F})$ was placed physically close to the RTD so that the performance of the circuit is not influenced by the dc biasing circuit, acting as a short circuit for the RF signals generated by the RTD-LD HIC.

The electrical circuit schematic of the RTD-LD HIC is illustrated in Fig. 2, where the dc biasing circuit is represented by a dc voltage source in series with a resistance R_b and a inductance L_b. The inductance L represents the overall inductance due to the microstrip line and the bond wire connections; R_{out}
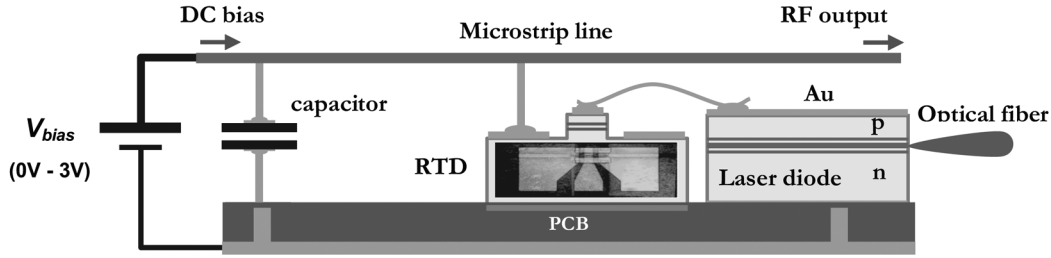
Fig. 1. Representation of the electrical connections on the PCB. The estimated inductance due to the microstrip line and bond wire connections from the PCB to the RTD and from the RTD to the laser is 8 nH.
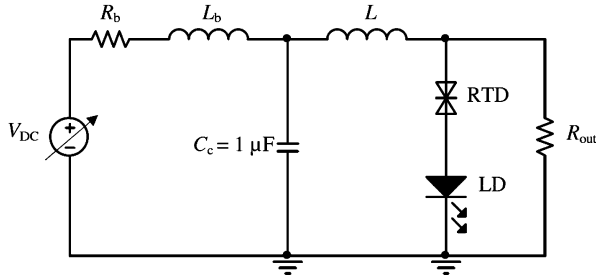

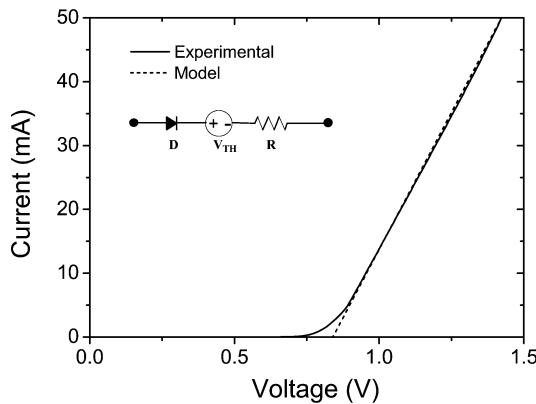Fig. 2. Schematic of the RTD-LD HIC equivalent circuit.

Fig. 3. Experimental and model I–V characteristics for the laser diode. Inset is the laser diode large signal model: an ideal diode in series with a voltage source and a current-limiting resistor.

Fig. 4. Experimental and model I–V characteristics for the RTD-LD HIC.

accounts for the impedance of the measuring instruments, 50 Ω in this case.

The laser diode was a commercial prototype device of the ridge waveguide design and was supplied by Compound Semiconductor Technologies Global Ltd. The laser was designed for continuous-wave (CW) room temperature operation and had an emission wavelength of 1550 nm, a bandwidth of 20 GHz and a threshold current of 6 mA. Fig. 3 shows the laser diode experimental I–V characteristic. When operated above the threshold, the laser can be modeled using an ideal diode in series with a voltage source V_{TH} and a current-limiting resistor R_S. From Fig. 3 we obtain $V_{TH} = 0.84$ V and $R_S = 11$ Ω.

The RTD component of the RTD-LD HIC was fabricated from RTD epi-material that was originally used in the work described in [1]. The InGaAlAs RTD structure was grown by molecular beam epitaxy in a Varian Gen II system on a n^+ InP substrate. It essentially consisted of two 2-nm-thick
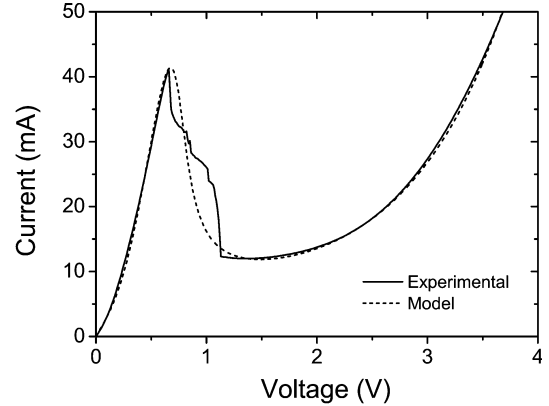
AlAs barriers separated by a 6-nm-wide InGaAs quantum well. A δ-doped InGaAs cap layer was provided for formation of Au–Ge–Ni ohmic contacts. Ridges were fabricated by wet-etching after which ohmic contacts were deposited on top of the ridges. A SiO$_2$ layer was then deposited, and access contact windows were etched on the ridge electrodes allowing contact to be made to high frequency bonding pads (coplanar waveguide transmission lines). The experimental RTD I–V characteristic is shown in Fig. 4 and fitted using the physics based description of the RTD given by [10]

$$f(V) = A \ln \left[\frac{1 + e^{q(B-C+n_1 V(t))/k_B T}}{1 + e^{q(B-C-n_1 V(t))/k_B T}} \right]$$
$$\cdot \left[\frac{\pi}{2} + \tan^{-1} \left(\frac{C - n_1 V(t)}{D} \right) \right]$$
$$+ H \left(e^{n_2 q V(t)/k_B T} - 1 \right) \qquad (1)$$

where $I = f(V)$ and using the fitting parameters $A = 6.48 \times 10^{-3}, B = 0.0875, C = 0.1449, D = 0.02132, H = 7.901 \times 10^{-4}, n_1 = 0.1902, n_2 = 0.0284$, and $T = 300$ K; q and k_B are the electric charge and the Boltzmann constant, respectively.

The RTD-LD HIC was biased using a variable DC voltage supply producing self-sustained oscillations when biased in the NDR region. The oscillation frequency was controlled either by altering the inductance, L, which corresponds to a change in distance between the shunt capacitor and the RTD, Fig. 2, or by adjusting the bias point. From the RF output (Fig. 1), oscillations were observed in the time domain using a high bandwidth Tektronix sampling oscilloscope and in the frequency domain using a Hewlett Packard 8564E 40 GHz spectrum analyzer.
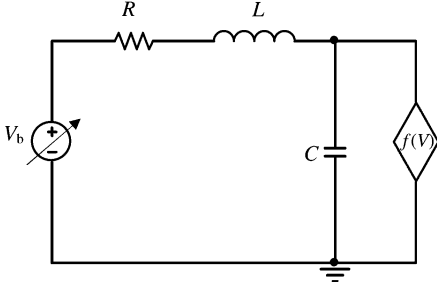
Fig. 5. Equivalent lumped circuit of the circuit shown in Fig. 2.

The current through the RTD-LD branch of the circuit acts to drive the laser diode, and its optical output oscillates with the same periodicity as the circuit oscillations. The optical signal was coupled from the laser diode into a lensed fibre connected to a 45 GHz bandwidth New Focus detector, the electrical output of which was observed in the frequency and time domain as for the RF circuit output.

III. THEORY AND NUMERICAL MODEL

For purposes of analysis and simulation, the circuit presented in Fig. 2 can be reduced to the circuit of Fig. 5, because the shunt capacitor C_c acts as a short circuit at the frequencies under consideration. In Fig. 5 the laser diode was replaced by a voltage drop and a series resistance (see Fig. 3), which is already included in the R and V_b circuit parameters. The RTD is represented by the voltage dependent current source $f(V)$, C is the RTD capacitance, R is the equivalent resistance of the RTD and LD, measuring instruments and connection wires, and L is the overall inductance due to the bond wires and microstrip.

Using Kirchhoff's rules the lumped circuit of Fig. 5 can be described by the following differential equations:

$$\frac{dV(t)}{dt} = \frac{i(t) - f(V)}{C} \tag{2}$$

$$\frac{di(t)}{dt} = \frac{V_b - Ri(t) - V(t)}{L} \tag{3}$$

where $V_b = V_{DC} - V_{TH}$ and V_{DC} is the dc bias voltage, $i(t)$ is the current through R and L, and $V(t)$ is the voltage across the RTD.

In NDR oscillator circuit models the voltage dependent current $I = f(V)$ of the NDR component is usually represented by a third order polynomial function $f(V) = aV^3(t) - bV(t)$. The substitution of $f(V) = aV^3(t) - bV(t)$ in the equations above gives, after some algebraic manipulation, the normalized Van der Pol equation [5]

$$\frac{d^2x}{dt^2} + u(x^2 - 1)\frac{dx}{dt} + x = 0 \tag{4}$$

where parameter u describes the nonlinear damping of the oscillator.

However, we found that a third order polynomial description was too restrictive to allow an accurate fitting of our experimental RTD I–V characteristic (Fig. 3), and so we adopted the more general representation given by (1), [10]. The substitution of $f(V)$ given by (1) shows, after algebraic manipulation, that

the time-dependent voltage across the RTD, $V(t)$, is then governed by the following second-order differential equation:

$$\frac{d^2V(t)}{dt^2} + h(V)\frac{dV(t)}{dt} + g(V) = 0 \tag{5}$$

where

$$h(V) = \frac{R}{L} + \frac{1}{C}\frac{df(V)}{dV} \tag{6}$$

$$g(V) = \frac{V(t)}{LC} + \frac{R}{LC}f(V) - \frac{V_{DC} - V_{TH}}{LC}. \tag{7}$$

Equation (5) is known as a kind of Liénard's oscillator [9], where $h(V) \cdot dV(t)/dt$ is the damping factor and $g(V)$ is the nonlinear force. This equation can be written in the more general form of the Liénard's oscillator nonlinear second order differential equation

$$\frac{d^2x}{dt^2} + h(x)\frac{dx}{dt} + g(x) = 0. \tag{8}$$

The solutions to this equation and the conditions on $h(x)$ and $g(x)$ have been discussed previously (see for example [9]). The Van der Pol equation, (4) is a particular form of the Liénard's equation with $h(x) = u(x^2 - 1)$ and $g(x) = x$, where u describes the nonlinear damping of the oscillator.

Numerically solving (5) gives through (2) the current through the laser, which is used to study the laser dynamics. The laser diode optical output can then be modeled using the laser diode single mode rate equations for the electron density N and the photon density S [11]

$$\frac{dN}{dt} = \frac{i(t)}{q\vartheta} - \frac{N}{\tau} - g_0(N - N_0)\frac{S}{1 + \varepsilon S} \tag{9}$$

$$\frac{dS}{dt} = g_0(N - N_0)\frac{S}{1 + \epsilon S} - \frac{S}{\tau_p} + \frac{\beta N}{\tau} \tag{10}$$

where $i(t)$ is the current through the laser given by Liénard's model, q is the electron charge, ϑ is the active region volume, τ and τ_p are the spontaneous electron and photon lifetime, β is the spontaneous emission factor, g_0 is the gain coefficient, N_0 is the minimum electron density required to obtain a positive gain and ϵ is the value for the nonlinear gain compression factor.

In next section we show how the electrical operation of the RTD-LD HIC can be analysed as a Liénard oscillator. Equation (5) is solved numerically using standard software packages such as Mathematica [12], and the modeling results are compared with the RTD-LD HIC experimental data. The laser optical output experimental data is fitted with the calculated light intensity as a function of the injection current $i(t)$ using the coupled rate equations (9) and (10).

IV. EXPERIMENTAL RESULTS AND COMPARISON WITH THE NUMERICAL MODEL

We now go on present the results and modeling from the RTD-LD HIC. Additionally, we describe recently obtained results from a low inductance version of the RTD-LD HIC designed for higher frequency operation.

Fig. 6 shows a typical experimental self-sustained oscillation in the the voltage at the circuit RF output when the bias point was 1.8 V; the oscillation fundamental frequency is 560 MHz. For comparison in the same figure is also shown the voltage
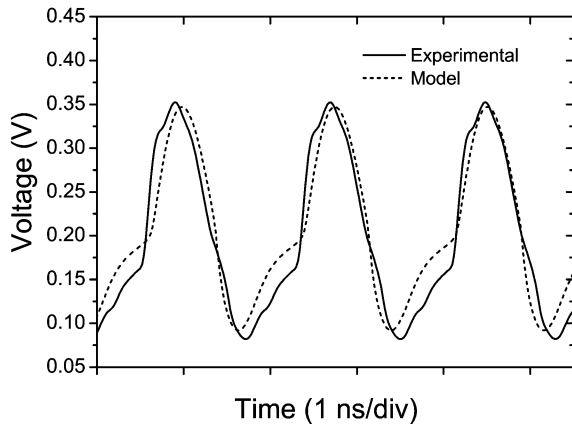
Fig. 6. Experimental and modeled electrical signal in the time domain at a bias of 1.8 V, both with a fundamental oscillation frequency of 560 MHz. The modeled signal has been scaled by a factor of 0.11 to fit the amplitude of the experimental signal.
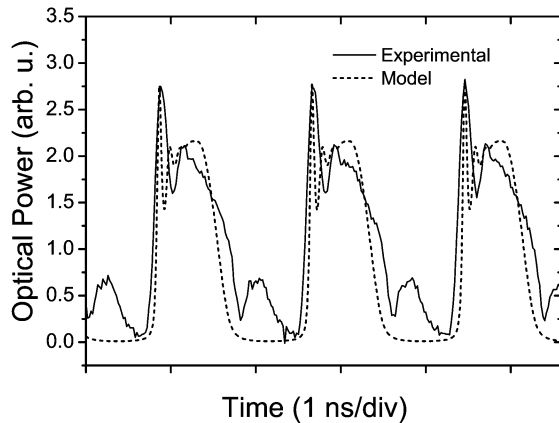

Fig. 7. Experimental and modeled laser optical output in the time domain at a bias of 1.8 V, both with a fundamental oscillation frequency of 560 MHz.
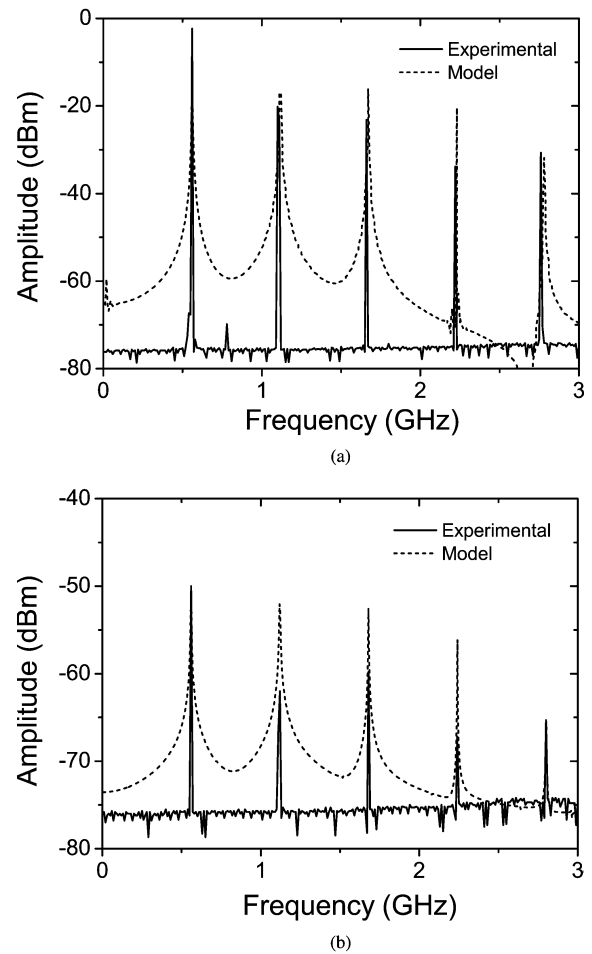

(a)

(b)

Fig. 8. Experimental and modeled (a) electrical and (b) optical RF signal spectra, both with a fundamental frequency of 560 MHz at a bias of 1.8 V. (a) RF spectrum of the electrical signal. (b) RF spectrum of the optical signal.

signal given by Liénard's model (5). The global circuit parameters used in the simulation are $L = 8.0$ nH, $C = 5.0$ pF, $R = 6.2\ \Omega$ and $V_{DC} = 1.8$ V.

The photo-detected signal, corresponding to the laser optical output, is shown in Fig. 7 together with the result obtained using (9) and (10). The laser dynamics are modeled employing typical parameters of semiconductor laser diodes [11], [13], with small adjustments to fit with experimental results $\vartheta = 6.75 \times 10^{-11}$ cm^3, $\tau = 2$ ns, $\tau_p = 1.2$ ps, $\beta = 3 \times 10^{-2}$, $g_0 = 10^{-6}$ cm^3/s, $N_0 = 10^{18}$ cm^{-3}, and $\epsilon = 0.6 \times 10^{-17}$ cm^3. As mentioned above, the repetition rate of the laser optical output was the same as the electrical circuit oscillation, clearly demonstrating that the laser diode operation was controlled by the RTD switching characteristics.

Fig. 8(a) and (b) show the experimental and modeled spectra (Fourier transform of time domain model) of the RTD-LD HIC electrical and optical outputs for a dc bias of 1.8 V. The RF spectrum of the photo-detector signal indicates that the laser output is modulated by the electrical self-sustained oscillation by an amount greater than 20 dB. The spectra predicted by the Liénard's model and the laser dynamics single mode rate equations

presented above seem to describe reasonably well the experimental behaviour of the RTD-LD HIC.

As discussed in Section II, the RTD-LD HIC acted as voltage controlled oscillator. Oscillation frequency increased from 350 MHz at a bias of 1.82 V to 398 MHz at a bias of 1.98 V for the circuit in the increased inductance configuration with the shunt capacitor positioned 20 mm along the microstrip from the RTD. For the capacitor positioned 5 mm from the RTD, the oscillation frequency increased from 550 MHz at 1.78 V to 590 MHz at 1.95 V. Fig. 9 shows the tuning curve for the circuit in the higher inductance configuration along with the modeling results. The Liénard's model approach given by (5), based on (1), is in good agreement with the experimental results. Our numerical analysis also shows the Van der Pol model based on the polynomial approximation to the RTD *I–V* characteristic does not reproduce the experimental tuning characteristic over the full range of frequencies.

We now present the experimental results and modeling from a second RTD-LD HIC, fabricated with the aim of achieving a higher oscillation frequency than that of the original RTD-LD HIC. The original RTD-LD HIC demonstrated increased oscillation frequency with reduced inductance, and to this end bond wire length was reduced to ∼1 − 2 mm (down from
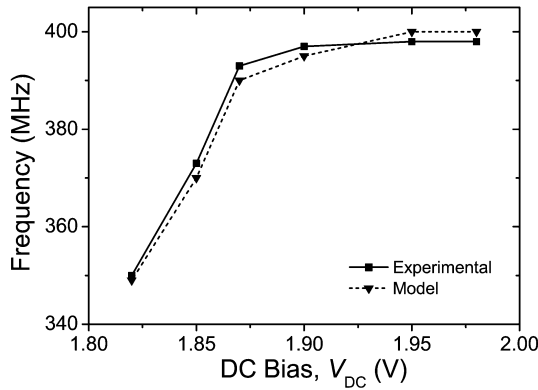
Fig. 9. Experimental and model tuning curve.

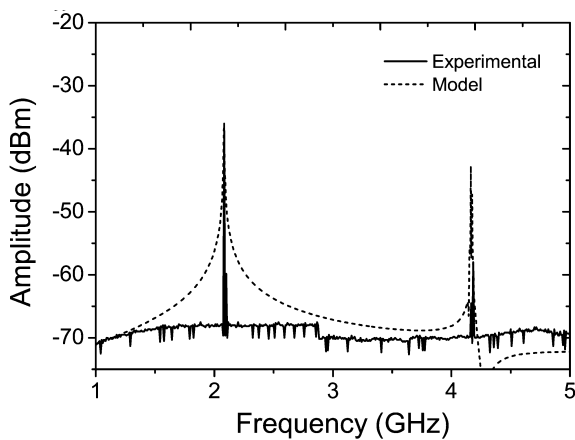Fig. 11. Experimantal and model tuning curve for the low inductance RTD-LD HIC.

Fig. 10. Experimental and modeled optical signal spectra for the low inductance RTD-LD HIC, with a fundamental frequency of 2.08 GHz at a bias of $V_{\mathrm{DC}} = 1.76$ V.

V. CONCLUSION

A hybrid integrated RTD-LD circuit (the RTD-LD HIC) acting as an oscillator producing both electrical and optical outputs has been built and characterized. The electrical and optical outputs have been measured in both the time and frequency domains. By numerically solving a second order nonlinear differential equation and obtaining a reasonably good fit to the optical and electrical results in both the time and frequency domains we have shown that the operation of the circuit can be described by Liénard's oscillator theory.

The RTD-LD HICs presented here operate at frequencies up to 2.1 GHz. With fully integrated versions we anticipate much higher operating frequencies in the region of 10 Gbits or higher—data rates more appropriate for present day optical communication systems.

The applications of this RTD-LD HIC Liénard's oscillator, or variants based on it, in optical communication systems include for example: 1) operation as a forced oscillator driven by a digital data source; 2) acting as a clock recovery circuit; 3) for direct data encoding using small perturbation signals to control the RTD-LD HIC [14]; and 4) for communications using chaotic waveforms [15]–[17].

~5 mm) using an improved circuit layout. Fig. 10 shows the optical spectra along with the results of modeling. The circuit oscillations have a fundamental frequency of 2.08 GHz and are essentially sinusoidal. The circuit exhibited voltage controlled tuning from 1.82 GHz at 1.73 V to 2.17 GHz at 1.79 V as shown in Fig. 11. The model was fitted to the RF Spectrum of the optical signal and tuning curve using the following estimated circuit parameters $L = 1.5$ nH, $C = 3$ pF and $\mathrm{R} = 4.5\ \Omega$ and employing the same laser diode fitting parameters. There was good agreement between model and experiment, demonstrating the validity of the Liénard's model at higher frequencies.

The comparison between the experimental results with the numerical simulation shows that the theory of the Liénard's nonlinear differential equations can be used to model a driver circuit for an optical communications semiconductor laser. Currently underway is a detailed study of the RTD-LD HIC nonlinear behaviour when an external sinusoidal voltage signal is applied. Under these conditions this non-autonomous circuit outputs various optical and electrical signal patterns that include frequency division, quasi-periodic oscillations, and generation of chaotic signals with potentially important applications in optical communication systems. Preliminary simulation shows the circuit non-linear dynamical performance can also be well described using Liénard's theory.
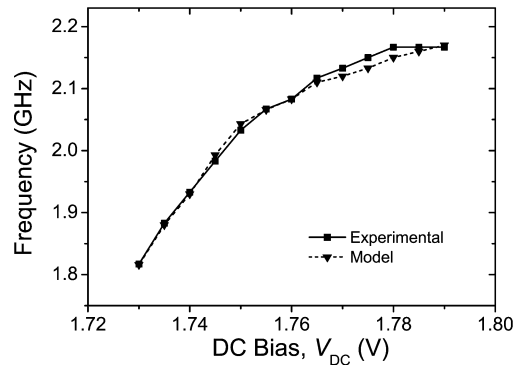
REFERENCES

[1] J. M. L. Figueiredo, C. N. Ironside, and C. R. Stanley, "Electric field switching in a resonant tunneling diode electroabsorption modulator," *IEEE J. Quantum Electron.*, vol. 37, no. 12, pp. 1547–1552, Dec. 2001.
[2] T. J. Slight and C. N. Ironside, "Investigation into the integration of a resonant tunnelling diode and an optical communications laser: Model and experiment," *IEEE J. Quantum Electron.*, vol. 43, no. 7, pp. 580–587, Jul. 2007.
[3] M. Asada, N. Orihashi, and S. Suzuki, "Experiment and theoretical analysis of voltage-controlled sub-THz oscillation of resonant tunneling diodes," *IEICE Trans. Electron.*, vol. E89C, no. 7, pp. 965–971, 2006.
[4] S. G. Zhou, M. Sweeny, J. M. Xu, and O. Berolo, "Chaotic behavior of quantum resonant tunneling diodes," *Physica D.*, vol. 52, no. 2–3, pp. 544–550, 1991.

[5] Z. Z. Sun, S. Yin, X. R. Wang, J. P. Cao, Y. P. Wang, and Y. Q. Wang, "Self-sustained current oscillations in superlattices and the Van der Pol equation," *Appl. Phys. Lett.*, vol. 87, no. 18, p. 182110, 2005.

[6] E. S. Hellman, K. L. Lear, and J. S. Harris, "Limit-cycle oscillation in negative differential resistance devices," *J. Appl. Phys.*, vol. 64, no. 5, pp. 2798–2800, 1988.

[7] E. V. Appleton and B. Van der Pol, "On a type of oscillation-hysteresis in a simple triode generator," *Philosoph. Mag.*, ser. 6, vol. 43, no. 253, pp. 177–193, 1922.

[8] J. Guckenheimer, "Dynamics of the Van der Pol equation," *IEEE Trans. Circuits Syst.*, vol. 27, no. 11, pp. 983–989, Nov. 1980.

[9] R. J. P. Figueiredo, "Existence and uniqueness results for Liénard's equation," *IEEE Trans. Circuit Theory*, vol. CT17, no. 3, p. 313, Jun. 1970.

[10] J. N. Schulman, H. J. D. Santos, and D. H. Chow, "Physics-based RTD current-voltage equation," *IEEE Electron Device Lett.*, vol. 17, no. 5, pp. 220–222, May 1996.

[11] P. V. Mena, S. Kang, and T. A. DeTemple, "Rate-equation-based laser models with a single solution regime," *J. Lightw. Technol.*, vol. 15, no. 4, pp. 717–730, 1997.

[12] R. H. Enns and G. C. McGuire, *Nonlinear Physics with Mathematica for Scientists and Engineers.* Boston, MA: Birkhuser, 2001.

[13] B. P. C. Tsou and D. L. Pulfrey, "A versatile SPICE model for quantumwell lasers," *IEEE J. Quantum Electron.*, vol. 33, no. 2, pp. 246–254, Feb. 1997.

[14] K. Maezawa, "A new generation of negative-resistance devices-new developments in ultrahigh-frequency applications based on resonant tunneling elements," *Electron. Commun. Jpn. Part II- Electron.*, vol. 89, no. 4, pp. 29–38, 2006.

[15] S. Hayes, C. Grebogi, E. Ott, and A. Mark, "Experimental control of chaos for communication," *Phys. Rev. Lett.*, vol. 73, no. 13, pp. 1781–1784, 1994.

[16] G. D. VanWiggeren and R. Roy, "Optical communication with chaotic waveforms," *Phys. Rev. Lett.*, vol. 81, no. 16, pp. 3547–3550, 1998.

[17] A. Argyris, D. Syvridis, L. Larger, V. Annovazzi-Lodi, P. Colet, I. Fischer, J. Garcia-Ojalvo, C. R. Mirasso, L. Pesquera, and K. A. Shore, "Chaos-based communications at high bit rates using commercial fibre-optic links," *Nature*, vol. 438, no. 7066, pp. 343–346, 2005.
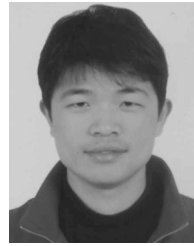
Thomas J. Slight received the B.Eng. degree in physics and electronic engineering and the Ph.D. degree in electronic engineering from the University of Glasgow, Glasgow, U.K., in 2002 and 2006, respectively.

He is currently with the Department of Electronics and Electrical Engineering, University of Glasgow, where his research interests include optoelectronic integrated circuits utilising resonant tunnelling diodes and short wavelength quantum cascade lasers for gas sensing.

Bruno Romeira was born in Portugal in 1982. He received the diploma degree in physics and chemistry from the University of Algarve, Faro, Portugal, in 2006. Since 2006, he as been with the Centre for Electronics Optoelectronics and Telecommunications (CEOT), Faro, Portugal where he is currently pursuing the Ph.D. degree in optoelectronic integrated circuits incorporating resonant tunneling devices.

His research interests include physics of low-dimensional semiconductor structures and the numerical simulation of electronic and optoelectronic circuits containing nonlinear devices.

Liquan Wang was born in China in 1981. He received the M.Sc. degree in electronics and electrical engineering from the University of Glasgow, Glasgow, U.K., in 2006, where he is currently pursuing the Ph.D. degree on the reliable design of microwave and millimeter-wave oscillators using tunneling diodes and resonant tunneling diodes (RTD).

Mr Wang's research interests include understanding RTD-driven laser diode circuits and associated applications.

José M. L. Figueiredo was born in Barcelos, Portugal. He received the B.Sc. degree in physics (optics and electronics) in 1991, and the M.Sc. degree in optoelectronics and lasers in 1995, both from the University of Porto, Portugal.

From 1995 to 1999, he was with the Department of Physics at the University of Porto and the Department of Electronics and Electrical Engineering at the University of Glasgow, U.K., as a Ph.D. student working on the optoelectronic properties of resonant tunneling diodes. Presently, he is member of the Physics Department at the University of the Algarve. His current research interests include the design and characterization of electronic and optoelectronic devices incorporating low dimensional quantum structures, and optoelectronic integrated circuits for telecommunications. He is also interested on optical remote sensing technologies.

Edward Wasige received the B.Sc.(Eng.) degree in electrical engineering from the University of Nairobi, Nairobi, Kenya, in 1988, the M.Sc.(Eng.) degree in microelectronic systems and telecommunications from the University of Liverpool, Liverpool, U.K., in 1990, and the Dr.-Ing. degree in electrical engineering from the University of Kassel, Kassel, Germany, in 1999.

During 1990–1993 and 1999–2001, he taught Electronics and Communications Engineering courses at Moi University, Eldoret, Kenya. Dr Wasige was a UNESCO Postdoctoral Fellow at the Technion—Israel Institute of Technology, Haifa, Israel, from May 2001 to August 2002, before joining the University of Glasgow, Glasgow, U.K., in September 2002. His current research interests include the reliable design of resonant tunneling diode microwave and millimeter-wave oscillators, and the development of new types of gallium nitride-based heterojunction field effect transistors for power electronics and microwave applications.

Charles N. Ironside has worked in the Department of Electronics and Electrical Engineering, University of Glasgow, Glasgow, U.K., since 1984, on a variety of optoelectronic projects that include, ultrafast all-optical switching in semiconductor waveguides, monolithic modelocked semiconductor lasers, broadband semiconductor lasers, quantum-cascade lasers and OptoElectronic Integrated Chip (OEIC) devices.

His OEIC work has concentrated on the integration of resonant tunnelling diodes with electroabsorption modulators and semiconductor lasers.